Commun. Theor. Phys. **72** (2020) 055501 (8pp) https://doi.org/10.1088/1572-9494/ab7701

Ion-acoustic waves at the night side of Titan's ionosphere: higher-order approximation

S M Ahmed[1], E R Hassib[1], U M Abdelsalam[2,3], R E Tolba[4] and W M Moslem[4,5,6]

[1] Department of Mathematics, Faculty of Science, Suez University, Suez, Egypt
[2] Department of Mathematics, Faculty of Science, Fayoum University, Fayoum, Egypt
[3] Department of Mathematics, Rustaq College of Education, Oman
[4] Centre for Theoretical Physics, The British University in Egypt (BUE), El-Shorouk City, Cairo, Egypt
[5] Department of Physics, Faculty of Science, Port Said University, Port Said 42521, Egypt

E-mail: samar_sohel@yahoo.com, mohmehab73@yahoo.com, usama.ahmad@rub.de, tolba_math@yahoo.com and wmmoslem@hotmail.com

Received 10 November 2019, revised 21 January 2020
Accepted for publication 22 January 2020
Published 2 April 2020

Abstract

Nonlinear solitary waves are investigated for a plasma system at the night side of Titan's ionosphere. The plasma model consists of three positive ions, namely $C_2H_5^+$, $HCNH^+$, and $C_3H_5^+$, as well as Maxwellian electrons. The basic set of fluid equations is reduced to a Korteweg de-Vries (KdV) equation and linear inhomogeneous higher order KdV (LIHO-KdV) equation. The solitary wave solutions of both equations are obtained using a renormalization method. The solitary waves' existence region and the wave profile are investigated, and their dependences on the plasma parameters at the night side of Titan's ionosphere are examined. The solitary waves' phase velocities are subsonic or supersonic, and the propagating pulses are usually positive. The effect of higher-order corrections on the perturbation theory is investigated. It is found that the higher-order contribution makes the amplitude slightly taller, which is suitable for describing the solitary waves when the amplitude augments.

Keywords: plasmas, ion-acoustic waves, planets and satellites: atmospheres

(Some figures may appear in colour only in the online journal)

1. Introduction

Titan is the largest moon of Saturn, which was discovered by Christiaan Huygens in 1655. It is considered the first known Saturn moon, and is known as the sixth planetary moon, after Earth's moon and the four Galilean satellites of Jupiter. It is the only moon with an intensive atmosphere in the solar system. Titan is the only object in space except the Earth where there is clear proof of the existence of stable bodies of surface liquid. Its atmosphere is composed of molecular nitrogen and methane, with minor amounts of many hydrocarbons and nitrile species [1]. In the solar system, Titan is the second-largest moon, where it comes in order after Jupiter's moon 'Ganymede', and it is larger than Mercury only by about 40%. Titan is 50% larger than the Earth's moon. The nature of the climate in Titan, such as wind and rain, possibly creates similar features to those found in the Earth as rivers, seas, lakes and deltas (most likely consisting of liquid methane and ethane), dominated by weather forms as on the Earth. Measurement data from the Cassini spacecraft, which has visited Saturn and its satellites since its arrival at the planet in 2004, has been analyzed and investigated by many authors [2–5].

Observations indicate that Titan's ionosphere structure may be the most complex in the solar system, with nearly 110 ions. Most of these ions are positive, but as a result of the chemical reaction, a small amount of negative ions have been observed in specific regions [6–8]. There are a reasonably

[6] Author to whom any correspondence should be addressed.

small number of negative ions; however, the chemistry study of the hydrocarbon atmospheres cannot neglect this inside the Moon's surface and the composition of Titan's aerosols. Observations show that the ionosphere of Titan is dominated by $HCNH^+$ and $C_2H_5^+$ ions with densities 4.6×10^2 cm^{-3} and $2 \times 10^2\,cm^{-3}$, respectively, whereas all the other ion species (in excess of 110 ion species) are present in densities varying from 10^{-7} up to a few tens per cm^3 [8]. Therefore, the upper ionosphere of Titan consists of 60% of $HCNH^+$ and C_2 H_5^+ ions only. Different flybys indicate that at different altitudes the ion concentration changes. For example, Cravens *et al* 2006 showed that at an altitude of ≈1300 km, the main ion components are $HCNH^+$, $C_2H_5^+$, and $C_3H_5^+$ [9].

In nonlinear dispersion media, the solitary waves appear because of the balance between the dispersion and the nonlinearity. The solitary pulses could be either positive or negative. Negative pulse is due to the density rarefaction, resulting in a rarefactive solitary wave, whereas positive dispersion due to the density compression gives rise to a compressive solitary pulse. Washimi and Taniuti (1966) first studied the propagation of ion-acoustic solitary waves (IASWs) in a simple plasma model by applying reductive perturbation theory to the basic equations governing the plasma dynamics. Later, many experimental and theoretical studies were carried out to examine the behavior of the IASWs in different plasma environments [10–14]. The aim of this manuscript is to investigate the properties of electrostatic nonlinear IASWs in a plasma containing three positive ions, and isothermal electrons at the night side of Titan's ionosphere.

The manuscript is organized as follows. In section 2, the reductive perturbation method is used to reduce the basic equations to an evolution equation called Korteweg–de Vries (KdV). As the wave amplitude increases, the width and velocity of the soliton deviate from the prediction of the KdV equation, i.e. the breakdown of the KdV approximation. To describe the soliton of larger amplitude, the higher-order KdV equation is derived. The stationary solutions of both KdV and higher-order KdV equations are obtained in section 3. In section 4, a parametric analysis of the solutions is performed using the observed data from the flybys. The results are summarized in section 5.

2. Formulation of the problem and derivation of evolution equations

Let us consider the propagation of small but finite amplitude ion-acoustic waves in an unmagnetized, collisionless plasma composed of three different positive ions, namely $C_2H_5^+$, $HCNH^+$, and $C_3H_5^+$ (referred to by the subscripts 1, 2, 3), as well as Maxwellian electrons (referred to by e). The dimensionless basic equations for moving ions are governed by

$$\frac{\partial n_i}{\partial t} + \frac{\partial (n_i u_i)}{\partial x} = 0, \tag{1}$$

$$\left(\frac{\partial}{\partial t} + u_i \frac{\partial}{\partial x}\right) u_i + \frac{3\sigma_i}{\mu_i} n_i \frac{\partial n_i}{\partial x} + \frac{1}{\mu_i}\frac{\partial \phi}{\partial x} = 0, \tag{2}$$

whereas the electrons are described by

$$n_e = N_e \exp(\phi). \tag{3}$$

Equations (1)–(3) are closed by the Poisson equation

$$\frac{\partial^2 \phi}{\partial x^2} = n_e - \sum_i n_i. \tag{4}$$

In equations (1)–(4) $i = 1, 2, 3$, the mass ratio $\mu_i = m_i/m_1$, where m_1, m_2, and m_3 are the masses of $C_2H_5^+$, $HCNH^+$, and $C_3H_5^+$ ions, respectively, $\sigma_i = T_i/T_e$. The dependent variables n_i and u_i are the densities and velocities of the three positive ions, ϕ is an electrostatic potential, x is the space coordinate, and t is the time variable. The densities are normalized by $n_1^{(0)}$, the distance is normalized by the Debye length $\lambda_{D1} = (k_B T_e/4\pi e n_1^{(0)})^{1/2}$, and the time is normalized by the ion plasma period $\omega_{p1}^{-1} = (m_1/4\pi e^2 n_1^{(0)})^{1/2}$, the electric potential is normalized by the thermal potential $k_B T_e/e$, and the velocities by the ion-sound speed $C_{s1} = (k_B T_e/m_1)^{1/2}$, where k_B, e, and T_e are the Boltzmann constant, electronic charge, and electron temperature, respectively.

In order to study the propagation of small but finite amplitude electrostatic perturbations for ion-acoustic waves, we employ the reductive perturbation method [15, 16]. This method suggests the following stretching space-time coordinates

$$\zeta = \varepsilon^{1/2}(x - \lambda t) \quad \text{and} \quad \tau = \varepsilon^{3/2} t, \tag{5}$$

where λ is the phase velocity to be determined later and ε is a small parameter ($\varepsilon \ll 1$). Furthermore, the dependent physical quantities in equations (1)–(4) are expanded as follows

$$n_i = N_i + \varepsilon n_i^{(1)} + \varepsilon^2 n_i^{(2)} + \varepsilon^3 n_i^{(3)} + ..., \tag{6a}$$

$$u_i = \varepsilon u_i^{(1)} + \varepsilon^2 u_i^{(2)} + \varepsilon u_i^{(3)} + ..., \tag{6b}$$

$$\phi = \varepsilon \phi^{(1)} + \varepsilon^2 \phi^{(2)} + \varepsilon^3 \phi^{(3)} + ..., \tag{6c}$$

where $N_e = \frac{n_e^{(0)}}{n_1^{(0)}}$, $N_2 = \frac{n_2^{(0)}}{n_1^{(0)}}$, and $N_3 = \frac{n_3^{(0)}}{n_1^{(0)}}$ are the normalized unperturbed density ratios. The quasi-neutrality condition at equilibrium reads

$$N_e - 1 - N_2 - N_3 = 0. \tag{7}$$

Substituting equations (5) and (6) into equations (1)–(4), we obtain to the lowest-order in ε the following relations

$$n_i^{(1)} = \frac{N_i^{(0)}}{\mu_i z_i}\phi^{(1)}, \quad u_i^{(1)} = \frac{\lambda}{\mu_i z_i}\phi^{(1)}, \tag{8a}$$

$$N_e = \sum_i \frac{N_i^{(0)}}{\mu_i z_i}, \tag{8b}$$

where $z_i = \lambda^2 - 3\sigma_i \frac{N_i^{(0)2}}{\mu_i}$. The next-order in ε gives

$$\lambda \frac{\partial n_i^{(2)}}{\partial \zeta} = \frac{\partial n_i^{(1)}}{\partial \tau} + \frac{\partial}{\partial \zeta}(N_i^{(0)} u_i^{(2)}) + \frac{\partial}{\partial \zeta}(n_i^{(1)} u_i^{(1)}), \tag{9a}$$

$$\lambda \frac{\partial u_i^{(2)}}{\partial \zeta} = \frac{\partial u_i^{(1)}}{\partial \tau} + u_i^{(1)} \frac{\partial}{\partial \zeta} u_i^{(1)} + \frac{3\sigma_i}{\mu_i} N_i^{(0)} \frac{\partial n_i^{(2)}}{\partial \zeta} + \frac{3\sigma_i}{\mu_i} n_i^{(1)} \frac{\partial n_i^{(1)}}{\partial \zeta} + \frac{1}{\mu_i}\frac{\partial \phi^{(2)}}{\partial \zeta}, \tag{9b}$$

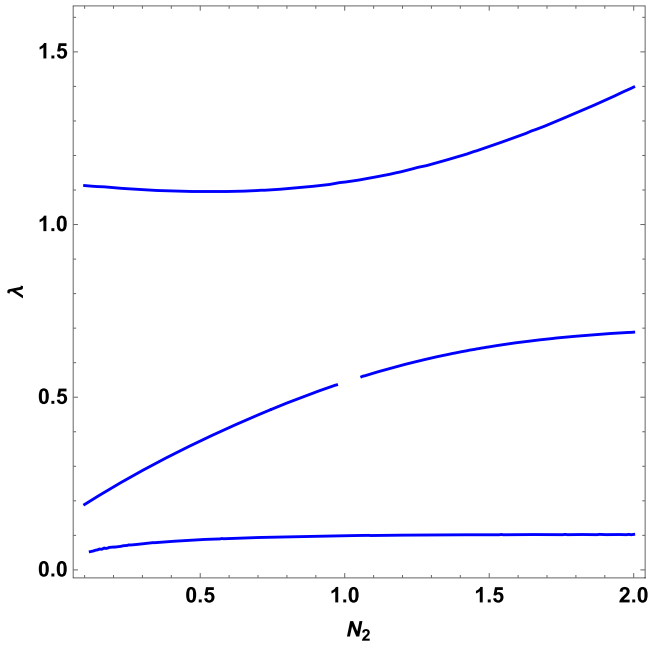

Figure 1. The phase velocity λ versus the density ratio N_2, where $\mu_2 = 0.97$, $\mu_3 = 0.68$, $\sigma_{1,2,3} = 0.1$, and $N_3 = 0.1$.

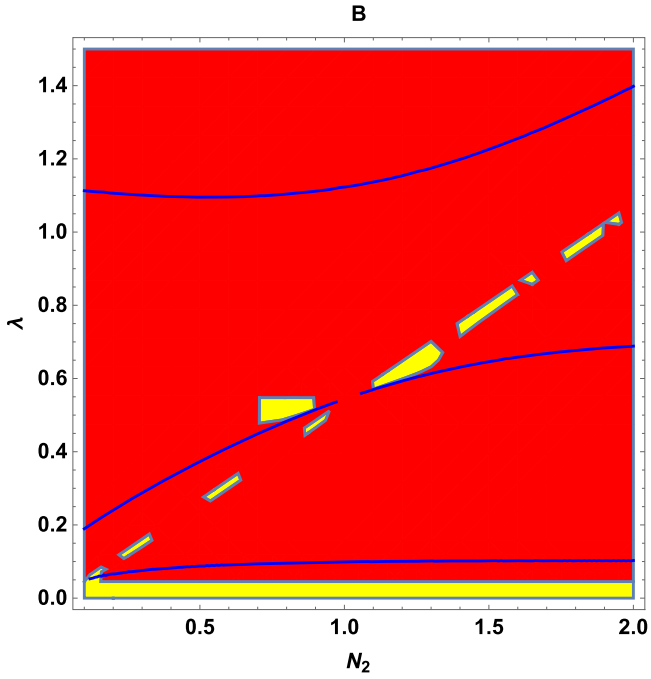

Figure 2. The polarity of the nonlinear term B versus N_2. The red region refers to the positive B while the yellow regions refer to negative B, and the blue lines refer to λ, where $\mu_2 = 0.97$, $\mu_3 = 0.68$, $\sigma_{1,2,3} = 0.1$, and $N_3 = 0.1$.

$$\frac{\partial^2\phi^{(1)}}{\partial\zeta^2} + \sum_i n_i^{(2)} = n_e^{(2)}. \tag{9c}$$

Solving equations (9) with the aid of equation (8), we finally obtain the Korteweg–de Vries (KdV) equation

$$\chi_1(\phi^{(1)})\phi^{(1)} = \frac{\partial\phi^{(1)}}{\partial\tau} + AB\phi^{(1)}\frac{\partial\phi^{(1)}}{\partial\zeta} + \frac{1}{2}A\frac{\partial^3\phi^{(1)}}{\partial\zeta^3} = 0, \tag{10}$$

where

$$A = \left[\sum_i \frac{\lambda N_i^{(0)}}{\mu_i z_i^2}\right]^{-1},$$

$$B = \frac{3}{2}\left[-\frac{1}{3}N_e + \sum_i \frac{N_i^{(0)}}{\mu_i^2 z_i^3}\left(z_i + \frac{4\sigma_i N_i^{(0)2}}{\mu_i}\right)\right].$$

It is interesting to examine the sign of the coefficients A and B. We use the data of Titan in Cravens *et al* 2006 at altitude $1000 \sim 1300$ km, where the main dominant species of ions are $HCNH^+$, $C_2H_5^+$, and $C_3H_5^+$ with densities about $300\,cm^{-3}$, $100\,cm^{-3}$, and $80\,cm^{-3}$, respectively. It is interesting to obtain the behavior of the phase velocity λ and its dependence on the density ratio (such as N_2). It is found from figure 1 that λ can be supersonic or subsonic (i.e. $\lambda > 1$ or $\lambda < 1$) depending on the value of density ratio N_2. We have noticed a broken line at $N_2 \approx 1$, which means that the value of λ is imaginary and the compatibility condition is not satisfied at these values of plasma parameters. It is clear from the definition of A that it is always positive, but B may be negative depending on the physical parameters. Keep in mind that we have to use the neutrality condition (7) and the compatibility condition (8b) into the coefficient B. Figure 2 shows that the regions where B may change its polarity versus λ and N_2. It is found that B is generally positive (red color regions) expect for small areas (indicated by the yellow color) which have a negative sign. However, the yellow zones do not satisfy the existence of λ (i.e. the compatibility condition (8b)) because λ does not pass through the yellow regions; it passes through the red region only. It means that the yellow (negative) B does not fulfill the compatibility condition (8b). Later, this condition clears that we have a positive (compressive) wave only, as we will show in the next section.

Equation (10) contains the lowest-order nonlinearity and dispersion. The main limitation of perturbation theory is that it can describe a wave of only small but finite amplitude. However, as the wave amplitude increases, the width and velocity of a solitary wave deviates from the prediction of the KdV equation (10), i.e. the KdV approximation fails to describe this situation. To describe the ion-acoustic solitary waves of larger amplitude, this has led us to consider the higher-order nonlinearity and dispersive. Therefore, the higher-order approximation of the reductive perturbation method is a powerful tool to provide adequate description of this case. Using equation (10) into (9) with the aid of the first-order results, we get

$$n_i^{(2)} = D_1\phi^{(1)2} + D_2\frac{\partial^2\phi^{(1)}}{\partial\zeta^2} + D_3\phi^{(2)}, \tag{11a}$$

$$u_i^{(2)} = E_1\phi^{(1)2} + E_2\frac{\partial^2\phi^{(1)}}{\partial\zeta^2} + E_3\phi^{(2)}, \tag{11b}$$

where D_i and E_i are given in the appendix.

The next-order of ε gives

$$\lambda\frac{\partial n_i^{(3)}}{\partial\zeta}=\frac{\partial n_i^{(2)}}{\partial\tau}+N_i^{(0)}\frac{\partial u_i^{(3)}}{\partial\zeta}+\frac{\partial}{\partial\zeta}(n_i^{(1)}u_i^{(2)})+\frac{\partial}{\partial\zeta}(n_i^{(2)}u_i^{(1)}),\tag{12a}$$

$$\lambda\frac{\partial u_i^{(3)}}{\partial\zeta}=\frac{\partial u_i^{(2)}}{\partial\tau}+\frac{\partial}{\partial\zeta}(u_i^{(1)}u_i^{(2)})+\frac{3\sigma_i\,N_i^{(0)}}{\mu_i}\frac{\partial n_i^{(3)}}{\partial\zeta}+\frac{3\sigma_i}{\mu_i}\frac{\partial}{\partial\zeta}(n_i^{(1)}n_i^{(2)})+\frac{1}{\mu_i}\frac{\partial\phi^{(3)}}{\partial\zeta},\tag{12b}$$

$$\frac{\partial^2\phi^{(2)}}{\partial\zeta^2}+\sum_i n_i^{(3)}=n_e^{(3)}.\tag{12c}$$

Solving equations (12) with the aid of equations (9) and (11), we obtain a linear inhomogeneous KdV-type equation for the second-order perturbed potential $\phi^{(2)}$ as

$$\begin{aligned}\chi_2(\phi^{(1)})\phi^{(2)}&=\frac{\partial\phi^{(2)}}{\partial\tau}+AB\frac{\partial}{\partial\zeta}(\phi^{(1)}\phi^{(2)})+\frac{1}{2}A\frac{\partial^3\phi^{(2)}}{\partial\zeta^3}\\&=-\left(H_1\phi^{(1)2}\frac{\partial\phi^{(1)}}{\partial\zeta}+H_2\frac{\partial\phi^{(1)}}{\partial\zeta}\frac{\partial^2\phi^{(1)}}{\partial\zeta^2}+H_3\phi^{(1)}\frac{\partial^3\phi^{(1)}}{\partial\zeta^3}+H_4\frac{\partial^5\phi^{(1)}}{\partial\zeta^5}\right),\end{aligned}\tag{13}$$

where H_{1-4} are given in the appendix. Thus, we have reduced the basic equations (1)–(4) to the KdV equation (10) for $\phi^{(1)}$ and a linear inhomogeneous KdV-type equation (13) for $\phi^{(2)}$. Solving equations (10) and (13) is the toolbox to describe the solitary wave either for lower or higher amplitudes, as we will discuss in the next section.

3. The stationary solutions

It is shown that the higher-order approximation is given by a linear inhomogeneous KdV-type equation (13) with an inhomogeneous term (a source term), but this equation has a resonant term that leads to secular solution. To remove the secular behavior, we apply the renormalization method [17, 18]. As a result of this method, we add equations (10) to (13) as

$$\chi_1(\phi^{(1)})\phi^{(1)}+\sum_{n\geqslant 2}\varepsilon^n\chi_2(\phi^{(1)})\phi^{(n)}=\sum_{n\geqslant 2}\varepsilon^n S_1^{(n)},\tag{14}$$

where $S_1^{(2)}$ is the source term and describes the right-hand side of equation (13). Adding $\varepsilon^n\ \delta\nu\frac{\partial\phi^{(n)}}{\partial\zeta}$ to both sides of equation (14). The important point in the method is that $\delta\nu$ on the right-hand side is only expanded, while it is not in the left-hand side. So that $\nu^{(n)}$ is specified to cancel out the resonant term in $S_1^{(n)}$. Therefore, we obtain

$$\frac{\partial\phi^{(1)}}{\partial\tau}+AB\phi^{(1)}\frac{\partial\phi^{(1)}}{\partial\zeta}+\frac{1}{2}A\frac{\partial^3\phi^{(1)}}{\partial\zeta^3}+\delta\nu\frac{\partial\phi^{(1)}}{\partial\zeta}=0,\tag{15}$$

$$\frac{\partial\phi^{(2)}}{\partial\tau}+AB\frac{\partial}{\partial\zeta}(\phi^{(1)}\phi^{(2)})+\frac{1}{2}A\frac{\partial^3\phi^{(2)}}{\partial\zeta^3}+\delta\nu\frac{\partial\phi^{(2)}}{\partial\zeta}=S_1^{(2)}(\phi^{(1)})+\delta\nu\frac{\partial\phi^{(1)}}{\partial\zeta}.\tag{16}$$

Equations (15) and (16) are the KdV and KdV-type equations in renormalized form.

The following independent variable

$$\eta=\zeta-(\nu+\delta\nu)\tau,\tag{17}$$

is introduced into equation (15) to give

$$-2\nu\phi^{(1)}+AB\phi^{(1)2}+A\frac{\mathrm{d}^2\phi^{(2)}}{\mathrm{d}\eta^2}=0.\tag{18}$$

We get the stationary soliton solution from equation (18), where we integrate equation (15) using the boundary conditions for $|\eta|\to\infty$ as

$$\phi^{(1)}=\phi^{(0)}\mathrm{sech}^2(\eta D),\tag{19}$$

where the maximum amplitude $\phi^{(0)}=3\nu/AB$ and the width $D=\sqrt{\nu/2A}$. Applying the same procedure to obtain the stationary solution of equation (16). Thus, it can be written as

$$-\frac{2\nu}{A}\phi^{(2)}+2B(\phi^{(1)}\phi^{(2)})+\frac{\mathrm{d}^2\phi^{(2)}}{\mathrm{d}\eta^2}=\frac{2}{A}\left[\int_{-\infty}^{\eta}S^{(2)}(\phi^{(1)})\mathrm{d}\eta+\delta\nu\phi^{(1)}\right].\tag{20}$$

The source term of (20), using (19), can be written as follows

$$\begin{aligned}&\frac{2}{A}\left[\int_{-\infty}^{\eta}S^{(2)}(\phi^{(1)})\mathrm{d}\eta+\delta\nu\phi^{(1)}\right]\\&=\frac{-2}{A}[2(H_2+H_3)\phi^{(0)2}D^2-120H_4\phi^{(0)}D^4]\,\mathrm{sech}^4(\eta D)\\&\quad-\frac{2}{A}\left[\frac{1}{3}H_1\phi^{(0)3}-2(H_2+2H_3)\phi^{(0)2}D^2\right.\\&\quad\left.+120H_4\phi^{(0)}D^4\right]\mathrm{sech}^6(\eta D),\end{aligned}\tag{21}$$

To remove the secular term, we put

$$\delta\nu=4H_4\nu^2/A^2,$$

to get the solution of (20) with the source term (21). Let that

$$\mu=\tanh\eta D.\tag{22}$$

Using equation (22) into (20), we obtain an associated inhomogeneous Legendre equation as

$$\frac{\mathrm{d}}{\mathrm{d}\mu}\left[(1-\mu^2)\frac{\mathrm{d}}{\mathrm{d}\mu}\phi^{(2)}\right]+\left[3(3+1)-\frac{2^2}{1-\mu^2}\right]\phi^{(2)}=T(\mu),\tag{23}$$

where

$$T(\mu)=H_5(1-\mu^2)+H_6(1-\mu^2)^2,$$

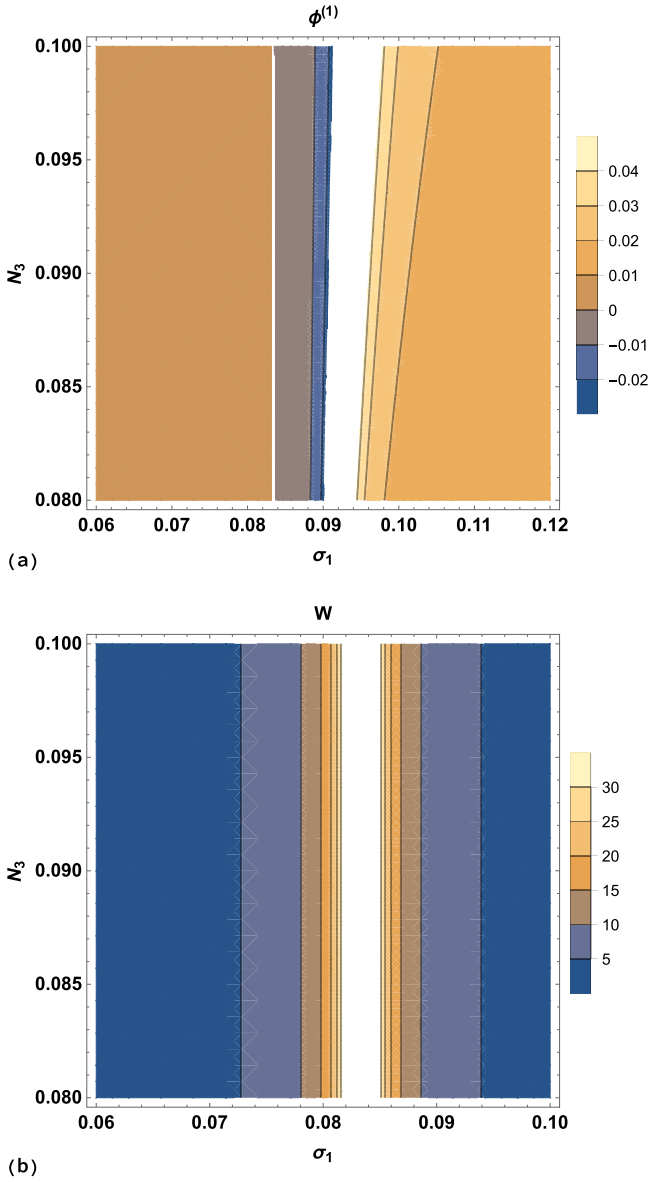

Figure 3. The contour plot of (a) the maximum amplitude $\phi^{(0)}$ and (b) the width W of the IASWs with N_3 and σ_1, where $\mu_2 = 0.97$, $\mu_3 = 0.68$, $N_2 = 0.25$, $\sigma_{2,3} = 0.1$, and $\lambda = 0.5$.

$$H_5 = -4\left[\frac{9}{A^3B^2}(H_2 + H_3) - \frac{90}{A^3B}\nu H_4\right],$$
$$H_6 = \frac{-2}{A}\left[\frac{27\nu^3}{3A^3B^3}H_1 - \frac{18\nu^2}{A^2B^2}(H_2 + 2H_3) + \frac{180\nu^2}{A^2B}H_4\right]. \quad (24)$$

The two independent solutions of the homogeneous part of equation (23) are given by the associated Legendre function of first and second kind:

$$P_3^2 = 15\mu(1-\mu^2), \quad (25)$$
$$Q_3^2 = \frac{15}{2}\mu(1-\mu^2)\ln\frac{1+\mu}{1-\mu} + 2\frac{\mu^2(5\mu^2-3)}{(1-\mu^2)} + 20\mu^2 - 8, \quad (26)$$

then the complementary solution of (23) is

$$\phi_c^{(2)} = C_1 15\mu(1-\mu^2) + C_2\left(\frac{15}{2}\mu(1-\mu^2)\ln\frac{1+\mu}{1-\mu} + 2\frac{\mu^2(5\mu^2-3)}{(1-\mu^2)} + 20\mu^2 - 8\right). \quad (27)$$

To get the particular solution of equation (23), by using the variation of parameters which can be written as

$$\phi_p^{(2)} = L_1(\mu)P_3^2(\mu) + L_2(\mu)Q_3^2(\mu), \quad (28)$$

where $L_1(\mu)$ and $L_2(\mu)$ are two functions of μ determined under some conditions. Substituting the solution (28) into equation (23), we get

$$L_1(\mu) = -\int \frac{Q_3^2 T(\mu)\mathrm{d}\mu}{(1-\mu^2)W(P_3^2, Q_3^2)} = \frac{1}{32}(1-\mu^2)^3\left[\frac{1}{3}H_5 + \frac{1}{4}H_6(1-\mu^2)\right] \times \ln\frac{1+\mu}{1-\mu} + \mu\left[\frac{11}{240}H_5 + \frac{49}{960}H_6\right] - \mu^3\left[\frac{1}{18}H_5 + \frac{73}{960}H_6\right] + \mu^5\left[\frac{1}{48}H_5 + \frac{11}{192}H_6\right] - \frac{1}{64}\mu^7 H_6,$$

$$L_2(\mu) = \int \frac{P_3^2 T(\mu)\mathrm{d}\mu}{(1-\mu^2)W(P_3^2, Q_3^2)} = \frac{-1}{16}(1-\mu^2)^3\left[\frac{1}{3}H_5 + \frac{1}{4}H_6(1-\mu^2)\right],$$

where the Wornkskian W is given by

$$W(P_3^2, Q_3^2) = P_3^2\frac{\mathrm{d}Q_3^2}{\mathrm{d}\mu} - Q_3^2\frac{\mathrm{d}P_3^2}{\mathrm{d}\mu} = \frac{120}{(1-\mu^2)}.$$

The particular solution of equation (23) can be written as

$$\phi_p^{(2)} = \left(\frac{1}{6}H_5 + \frac{1}{8}H_6\right)(1-\mu^2) + \frac{1}{8}H_6(1-\mu^2)^2. \quad (29)$$

As a result of the vanishing boundary condition the constant $C_2 = 0$ for $\phi_\eta^{(2)}$ as $|\eta| \to \infty$. The rest of $\phi_c^{(2)}$ is nothing but the secular term, which is eliminated by renormalization of the amplitude. Substituting (29) in terms of η, so the final solution of (23) is given by

$$\phi^{(2)} = \frac{9\nu^2}{A^3B^2}\left[\frac{5B}{3}H_4 - \frac{1}{6}H_2 + \frac{1}{3}H_3 - \frac{1}{AB}H_1\right]\mathrm{sech}^2(\eta D) + \frac{9\nu^2}{A^3B^2}\left[-\frac{1}{AB}H_1 + \frac{1}{2}H_2 + H_3 - 5BH_4\right] \times \mathrm{sech}^2(\eta D)\tanh^2(\eta D). \quad (30)$$

Thus, we finally obtain the total stationary solution $(\phi^{(1)} + \phi^{(2)})$ in terms of the variable η as

$$\phi = \frac{3\nu}{AB}\,\mathrm{sech}^{\,2}(\eta D) + \frac{9\nu^2}{A^3B^2}M_1\,\mathrm{sech}^{\,2}(\eta D) + \frac{9\nu^2}{A^3B^2}M_2\,\mathrm{sech}^{\,2}(\eta D)\tanh^{\,2}(\eta D), \tag{31}$$

where

$$M_1 = \left[\frac{5B}{3}H_4 - \frac{1}{6}H_2 + \frac{1}{3}H_3 - \frac{1}{AB}H_1\right],$$
$$M_2 = \left[-\frac{1}{AB}H_1 + \frac{1}{2}H_2 + H_3 - 5BH_4\right].$$

4. Numerical results and discussion

We recall that observations showed that Titan's ionosphere is composed of many ion species, depending on the altitude. For altitude 1000 $\sim$ 1300 km, there are three main dominant ion species, namely $HCNH^+$, $C_2H_5^+$, and $C_3H_5^+$, with densities about 300 cm^{-3}, 100 cm^{-3}, and 80 cm^{-3}, respectively [9]. From figure 2, we pointed out that B is always positive and from equation (19) the polarity of the maximum amplitude depends on the sign of B, which indicates that only positive solitary waves can exist. The yellow areas represent the regions that have rarefactive (negative) pulses, which are not physical since at these areas the compatibility condition is not fulfilled. Note that the blue lines pass only through the red zones. Thus, the compressive (positive) pulses can only propagate in our system. It is interesting to investigate the dependence of the solitary pulses profile (i.e. amplitude and width) on various plasma parameters, as well as the effect of higher-order perturbation correction as depicted in the following figures.

Figure 3 shows the soliton amplitude and width profile with the density ratio $N_3(=n_3^{(0)}/n_1^{(0)})$ and temperature ratio ($\sigma_1 = \sigma_2 = \sigma = T_i/T_e$). It is seen that the temperature ratio plays a significant role in changing the solitary pulse amplitude. On the other hand, for small $\sigma \leqslant 0.083$ the positive pulses amplitude decreases until it vanishes for the blue and brown regions of figure 3(a). For higher $\sigma \geqslant 0.09$ the positive pulses become shorter. The width of the solitary waves also changes with σ, which it increases for $\sigma \approx 0.085$ and then decreases for $\sigma > 0.085$. Note that the white zone indicates that the potential and width are very high compared to the colored regions. The mathematical program cannot match the colors for very low and very high values, so the anomalies' values take the white color. The effect of the density ratio of N_3 on the pulse width and amplitude is approximately negligible, so we do not include this behavior here.

Figure 4 shows the behavior of the density ratio N_2 and phase velocity λ with the solitary pulses' amplitude and width. It is seen that the amplitude has a complex behavior with λ and N_2 for small $\lambda < 0.5$, i.e. the amplitude significantly varies with the change of λ and N_2. However, for $\lambda > 0.5$ it does not change with N_2, but it slightly increases with λ. The solitary pulses' width has a straightforward behavior with λ and N_2. On the other hand, the pulses' width

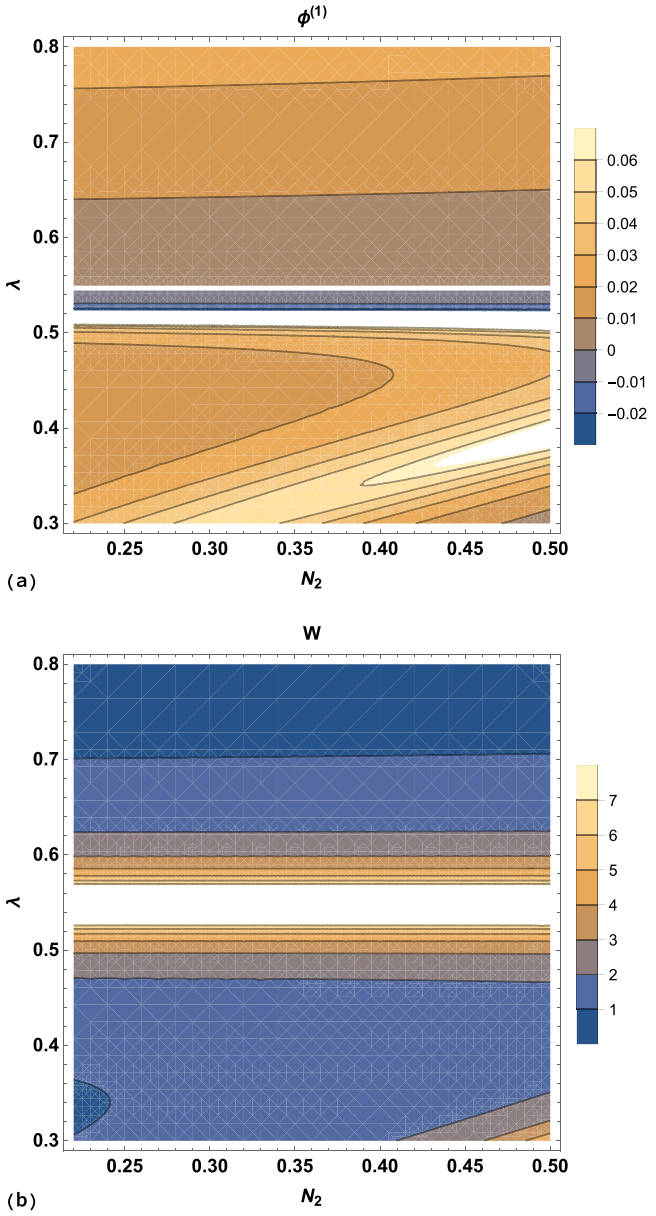

Figure 4. The contour plot of (a) the maximum amplitude $\phi^{(0)}$ and (b) the width W of the IASWs with N_2 and λ, where $\mu_2 = 0.97$, $\mu_3 = 0.68$, $N_3 = 0.1$, and $\sigma_{1,2,3} = 0.1$.

becomes wider for $\lambda < 0.55$, but becomes narrower for $\lambda > 0.55$. The effect of N_2 only changes the pulses' width for small $\lambda \leqslant 0.4$.

Finally, the effect of higher-order contribution on the perturbation theory is depicted in figure 5, i.e. we have plotted $\phi^{(1)}$ and $\phi^{(1)} + \phi^{(2)}$. It is obvious that the effect of higher order in the perturbation theory leads to slight enhancement of the amplitude, which indicates that as the wave amplitude increases, the width and velocity of the solitary wave deviates from the prediction of the KdV equation. The main reason to consider the high-order correction is that the usual KdV equation contains the lowest-order nonlinearity and dispersion, and consequently can describe a wave of only small amplitude. As the wave amplitude increases, the width and velocity of a soliton deviate from the prediction of the KdV

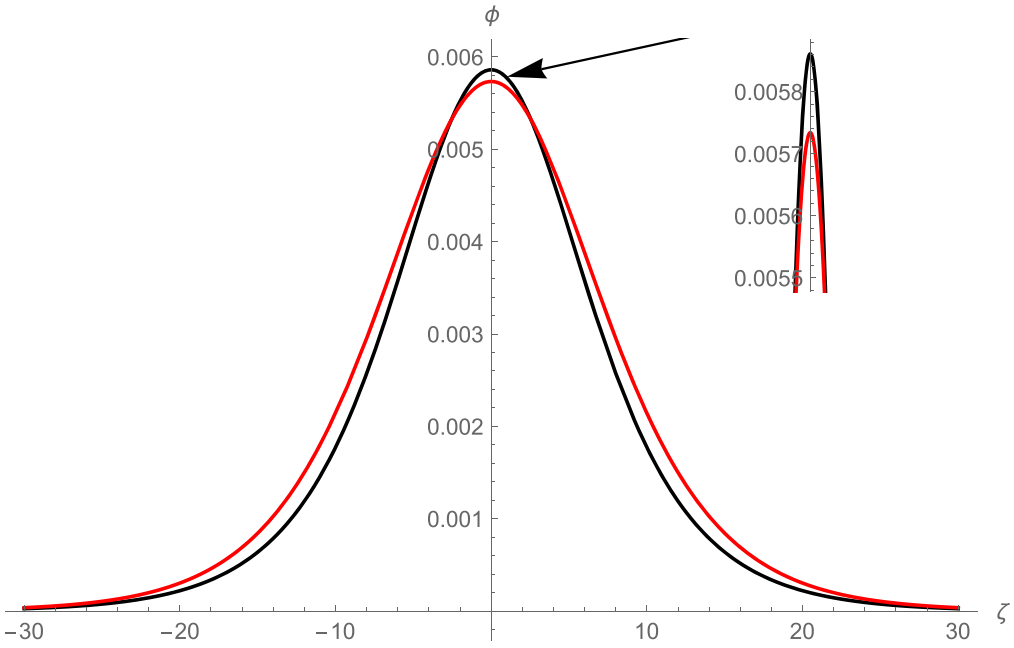

Figure 5. A graph of $\phi^{(1)}$ (red color) and $\phi^{(1)} + \phi^{(2)}$ (black color) versus ζ, where $\mu_2 = 0.97$, $\mu_3 = 0.68$, $N_2 = 0.22$, $N_3 = 0.1$, $\sigma_{1,2,3} = 0.1$, and $\lambda = 0.8$.

equation; thus it may lead to the breakdown of the KdV approximation. Therefore, to describe the soliton of larger amplitude, the higher-order nonlinearity and dispersion have to be taken into account, and the higher-order approximation of the reductive perturbation method has been known to be a powerful tool. In the present model, the higher-order correction has little effect, but in other models its effect may be influential. When we started this work we did not know the effect of higher-order correction, but after we performed the numerical analysis we found that the higher-order correction has minimal effect and we can conclude that the lower-order KdV is sufficient to describe the present physical phenomenon. Thus, we introduce this result to the readers as we found it. It may be that for other physical situations the effect of higher-order correction is significant; thus it should be taken into account to describe the phenomenon correctly and successfully.

5. Summary

We adopted a theoretical model appropriate for describing the nonlinear ion-acoustic solitary waves at the night side of Titan's ionosphere at altitude 1000 to 1400 km. The plasma model consists of three positive ions, namely $C_2H_5^+$, $HCNH^+$, and $C_3H_5^+$ ions, as well as Maxwellian electrons. The basic fluid equations are reduced to the KdV and a linear inhomogeneous KdV-type equations. The stationary solutions of these equations have been obtained using a renormalization method. We have numerically examined the existence regions for the solitary pulses and studied the relevance of the physical parameters to the amplitude and the width of the KdV soliton solution. It is found that the phase velocity of the propagating wave can be subsonic or supersonic. Furthermore, the propagating pulses are usually positive, and no negative pulses exist. The maximum amplitude and width of the solitary waves are affected by the density ratio between $HCNH^+$ and $C_2H_5^+$ (via N_2), temperature ratio between positive ions-to-electrons (via σ), and phase velocity λ. However, the the density ratio between $C_3H_5^+$ and $C_2H_5^+$ (via N_3) has no significant effect on the soliton profile. Finally, the effect of higher-order correction on the perturbation theory is investigated. It is seen that the higher-order contribution makes the amplitude slightly taller, which is suitable for describing the solitary wave when the amplitude increases, and therefore the width and velocity of the solitary wave deviates from the prediction of the KdV equation. The results presented here may be useful to have a deep understanding of the nonlinear electrostatic structures in Titan's lower ionosphere.

Appendix. Coefficients of equations (11) and (13)

$$D_1 = \frac{1}{2}\sum_i \left[\frac{3N_i^{(0)}}{\mu_i^2 z_i^3}\left(z_i + \frac{4\sigma_i N_i^{(0)2}}{\mu_i}\right) - 2\frac{\lambda N_i^{(0)}}{\mu_i\, z_i^2}AB\right],$$

$$D_2 = -\lambda A\sum_i \frac{N_i^{(0)}}{\mu_i z_i^2},$$

$$D_3 = A\sum_i \frac{N_i^{(0)}}{\mu_i z_i},$$

$$E_1 = \sum_i \frac{1}{2}\left[\frac{-1}{\mu_i z_i^2}\left(z_i + \frac{6\sigma_i N_i^{(0)2}}{\mu_i}\right)AB + \frac{1}{\lambda\mu_i^2 z_i^2}\left(z_i + \frac{6\sigma_i N_i^{(0)2}}{\mu_i}\right) + \frac{9\sigma_i N_i^{(0)2}}{\lambda\mu_i^3 z_i^3}\left(z_i + \frac{4\sigma_i N_i^{(0)2}}{\mu_i}\right)\right],$$

$$E_2 = -A\sum_i \frac{1}{2\mu_i^2 z_i^2}\left(z_i + \frac{6\sigma_i N_i^{(0)2}}{\mu_i}\right),$$

$$E_3 = \sum_i \frac{1}{\lambda\mu_i z_i}\left(z_i + \frac{3\sigma_i N_i^{(0)2}}{\mu_i}\right),$$

$$H_1 = \frac{1}{2}A\sum_i \left\{\left[\frac{3}{z_i^2}\left(\lambda^2 + \frac{3\sigma_i N_i^{(0)2}}{\mu_i}\right) - \frac{2\lambda}{\mu_i z_i}AB\right]D_1 + \left[\frac{2N_i^{(0)}}{\mu_i z_i}\left(\frac{3\lambda}{z_i} - AB\right)\right]E_1\right\},$$

$$H_2 = \frac{1}{2}A\sum_i \left\{\left[\frac{1}{z_i^2}\left(\lambda^2 + \frac{3\sigma_i N_i^{(0)2}}{\mu_i}\right) - \frac{\lambda}{\mu_i z_i}AB\right]D_2 + \left[\frac{N_i^{(0)}}{\mu_i z_i}\left(\frac{2\lambda}{z_i} - AB\right)\right]E_2\right\},$$

$$H_3 = \frac{1}{2}A\sum_i \frac{A}{\mu_i z_i}\{-\lambda D_1 + \lambda B D_2 + N_i^{(0)} B E_2 - N_i^{(0)} E_1)\},$$

$$H_4 = -\frac{1}{4}A^2\sum_i \left\{\frac{\lambda}{\mu_i z_i}D_2 + \frac{N_i^{(0)}}{\mu_i z_i}E_2\right\}.$$

ORCID iDs

W M Moslem https://orcid.org/0000-0002-5540-5756

References

[1] Waite J H *et al* 2005 *Science* **308** 982
[2] Coates A J, Wellbrock A, Waite J H and Jones G H Jr 2015 *Geophys. Res. Lett.* **42** 4676
[3] Horst S M 2017 *Journal of Geophys. Res.: Planets.* **3** 432
[4] Salem S, Moslem W M and Radi A 2017 *Phys. Plasmas* **24** 052901
[5] Dubois D, Carrasco N, Bourgalais J, Vettier L, Desai R T, Wellbrock A and Coates A J 2019 *Astrophys. J. Lett.* **872** L31
[6] Coates A J, Crary F J, Lewis G R, Young D T, Waite J H and Sittler E C Jr 2007 *Geophys. Res. Lett.* **34** L22103
[7] Vuitton V, Lavvas P, Yelle R V, Galand M, Wellbrock A, Lewis G R, Coates A J and Wahlund J E 2009 *Planet. Space Sci.* **57** 1558
[8] Wellbrock A, Coates A J, Jones G H, Lewis G R and Waite J H Jr 2013 *Geophys. Res. Lett.* **40** 4481
[9] Cravens T E Jr 2006 *Geophys. Res. Lett.* **33** L07105
[10] Ikezi H, Taylor R J and Baker D R 1970 *Phys. Rev. Lett.* **25** 11
[11] Saleem H, Moslem W M and Shukla P K 2012 *J. Geophys. Res.* **117** A08220
[12] Abdelsalam U M 2013 *J. Plasma Phy.* **79** 287
[13] Abdelsalam U M and Zobaer M S 2018 *RMxAA* **54** 363
[14] Moslem W M, Rezk S, Abdelsalam U M and El-Labany S K 2018 *Adv. Space Res.* **61** 2190
[15] Washimi H and Taniuti T 1966 *Phys. Rev. Lett.* **17** 996
[16] El-Labany S K, Moslem W M and Safy F M 2006 *Phys. Plasmas* **13** 082903
[17] Kodama Y and Taniuti T 1978 *J. Phys. Soc. Jpn* **45** 298
[18] El-Labany S K and Moslem W M 2002 *Physica Scripta.* **65** 5